

Improved Side Weir Discharge Coefficient Modeling by Adaptive Neuro-fuzzy Methodology

Shahaboddin Shamshirband*, Hossein Bonakdari**, Amir Hossein Zaji***, Dalibor Petkovic****, and Shervin Motamedi*****

Received November 25, 2014/Revised 1st: April 24, 2015, 2nd: November 19, 2015/Accepted December 6, 2015/Published Online March 4, 2016

Abstract

In this article, the accuracy of a soft computing technique is evaluated in terms of discharge coefficient prediction of an improved triangular side weir. The process includes simulating the discharge coefficient with the Adaptive Neuro-Fuzzy Inference System (ANFIS). Matlab software is used for ANFIS modeling. To identify the most appropriate input variables, eight different input combinations with various numbers of inputs are examined. The performance of the proposed system is confirmed by comparing the ANFIS and experimental results for the testing dataset. The performance evaluation demonstrates that the ANFIS model with five inputs (Root Mean Square Error (RMSE) of 0.014) is more accurate than the ANFIS model with one input (RMSE = 0.088). The ANFIS model results are also compared with the results obtained from previous regression and soft computing studies.

Keywords: ANFIS, soft computing, discharge coefficient, triangular side weir, modeling, input combination

1. Introduction

Side weirs are among the most important structures used to divide and divert extra flow from main channels. The first mathematical investigation of side weirs was done by De Marchi (1934). The primary assumption was that the specific energy upstream and downstream of the side weir is equal. With this assumption, Eq. (1) was obtained to calculate the discharge variation along a side weir.

$$-\frac{dQ}{dx} = \frac{2}{3} Cd \sqrt{2g} (y-w)^{1/5} \quad (1)$$

where dQ/dx is the discharge variation along the side weir, Cd is the discharge coefficient, w is the weir height and y is the flow depth.

There are different types of side weirs, the most common form being rectangular (Nadesamoorthy and Thomson, 1972; Ranga Raju *et al.*, 1979; Singh *et al.*, 1994; Swamee *et al.*, 1994; Muslu, 2001; Ghodsian, 2003; Muslu *et al.*, 2003; Yuksel, 2004). Although rectangular side weirs have the least complex geometry and are therefore the easiest to construct, they are the least efficient at diverting flow from the main channel compared to modified side weirs (Bilhan *et al.*, 2011). When the tributary channel width has a limitation and the rectangular side weir cannot handle dividing

the flow, one of the most economical options is to use side weirs with modified shapes. Many studies have been conducted on side weirs with modified shapes, such as triangular, trapezoidal and elliptical. It has been concluded that the modified side weirs are 1.5 to 4.5 times more efficient than conventional rectangular side weirs (Kumar and Pathak, 1987; Cosar and Agaccioglu, 2004; Ghodsian, 2004; Emiroglu *et al.*, 2010; Aydin and Emiroglu, 2013; Mirnaseri and Emadi, 2013).

The complex nature of side weir characteristic prediction and high performance of soft computing methods has inspired a wide range of studies in this field (Bilhan *et al.*, 2010; Kisi *et al.*, 2012; Onen, 2014b, a). The basic concept of soft computing methodologies is to collect input/output data pairs and to learn the proposed network from these data. The neuro-fuzzy network, or adaptive Neuro-Fuzzy Inference System (ANFIS) (Jang, 1993) has been applied by several researchers for modeling (Khajeh *et al.*, 2009; Talei *et al.*, 2010; Petković and Čojbašić, 2011; Petković *et al.*, 2012, 2013a, 2013b; Ebtehaj and Bonakdari, 2014), making predictions (Dastorani *et al.*, 2010; El-Shafie *et al.*, 2011; Wahida Banu *et al.*, 2011; Wu and Chau, 2012) and control in various engineering systems. It is a hybrid intelligent system that merges the learning power of artificial neural networks with the knowledge representation of fuzzy logic.

*Senior Lecturer, Dept. of Computer System, Faculty of Computer Science and Information Technology, University of Malaya, 50603 Kuala Lumpur, Malaysia (E-mail: shamshirband@um.edu.my)

**Professor, Dept. of Civil Engineering, Razi University, Kermanshah, Iran (Corresponding Author, E-mail: bonakdari@yahoo.com)

***Ph.D. Candidate, Dept. of Civil Engineering, Razi University, Kermanshah, Iran (E-mail: amirzaji@gmail.com)

****Professor, University of Nis, Faculty of Mechanical Engineering, Dept. of Mechatronics and Control, Aleksandra Medvedeva 14, 18000 Nis, Serbia (E-mail: dalibortc@gmail.com)

*****Associate member, Institute of Ocean and Earth Sciences, University of Malaya, 50603, Kuala Lumpur, Malaysia (E-mail: Sherwin@um.edu.my)

The application of the ANFIS technique in side weir characteristic prediction has been investigated in numerous studies. Seyedian *et al.* (2014) used ANFIS to estimate the effect of length, flow depth and height of a rectangular side weir. The authors found that ANFIS could perform very well compared to the regression method in their investigations on side weir characteristics. Kisi *et al.* (2013) simulated the discharge coefficient of rectangular side weirs through ANFIS. The authors concluded that the ANFIS method is superior to linear and nonlinear regression in predicting the discharge coefficient of rectangular side weirs. Emiroglu and Kisi (2013) also used ANFIS for trapezoidal labyrinth side weirs and concluded that the ANFIS method was more accurate than the Artificial Neural Network (ANN). The ANFIS method was employed to predict the discharge coefficient of a semi-elliptical side weir by Dursun *et al.* (2012). The authors found that ANFIS was able to provide good estimation of the discharge coefficient for semi-elliptical side weirs.

In the current study, the ANFIS scheme is used to estimate the discharge coefficient of an improved triangular side weir. Matlab software is used for ANFIS modeling purposes. Eight different input combinations are examined with the ANFIS method to identify the most appropriate variables for simulating the discharge coefficient with high accuracy. The ANFIS model results are compared with previous findings (Borghei and Parvaneh, 2011; Zaji and Bonakdari, 2014) from discharge coefficient prediction for triangular side weirs based on the particle swarm optimization and nonlinear regression methods.

2. Materials and Method

2.1 Improved Side Weir Experimental Study

Data from Borghei and Parvaneh’s (2011) experimental study were used to train and test the current ANFIS models. The mentioned authors created an improved triangular side weir two times more efficient than simple side weirs. Fig. 1 shows a schematic overview of the improved side weir. The main channel of the experimental flume was made of glass, 0.4 m wide and 11 m long. To determine the effects of each parameter on the discharge coefficient, experiments were done with different weir lengths (L), weir included angles (θ), upstream Froude numbers (Fr_1) and upstream flow depths (y_1). The parameter variation

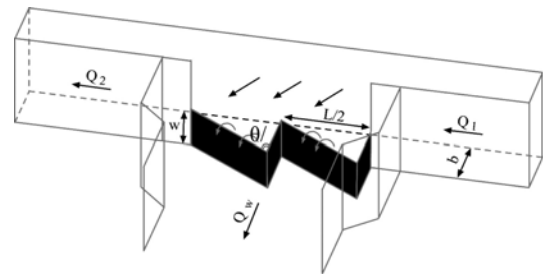


Fig. 1. Schematic Overview of the Improved Triangular Side Weir (Borghei and Parvaneh, 2011)

range in the experimental process is demonstrated in Table 1. Two hundred measurements were taken in different hydraulic and geometrical conditions. 50% of the entire dataset (100 samples) were randomly selected as the training dataset and the remaining samples comprised the testing dataset.

The head and discharge measurements were accurate up to ± 1 mm and ± 0.0001 m³/s, respectively.

2.2 Adaptive Neuro-fuzzy Application

ANFIS (Talei *et al.*, 2010; Petković *et al.*, 2013b) can serve as a basis for constructing a set of fuzzy ‘If-Then’ rules with an appropriate membership function to generate the stipulated input-output pairs. In this study, the ANFIS system used is functionally equivalent to a first-order Sugeno fuzzy model (Petković *et al.*, 2013b). A typical rule set with a fuzzy ‘If-Then’ rule can be expressed as

$$\text{if } x \text{ is } A \text{ then } f_i = p_i x + t \tag{2}$$

The ANFIS architecture with four inputs, x , y , z and j , is shown in Fig. 2. Nodes in the same layer have similar functions. The output of the i th node in layer l is denoted by $O_{l,i}$.

The first layer consists of the input variables’ Membership Functions (MFs) that supply the input values to the next layer. Every node i is an adaptive node with the node function:

$$O_{1,i} = \mu(x,y,z)_i \text{ for } i = 1, 2 \tag{3}$$

where x , y are the input to the i th node and $\mu(x,y,z)$ are membership functions.

The bell-shaped function can describe the MFs as:

Table 1. Variations of Experimental Parameters for the Improved Triangular Side Weir (Borghei and Parvaneh, 2011)

Number of runs	F_1	Q_i (m ³ /s)	w/Y_1	w (mm)	L (m)	$\theta/2$ (°)
40	0.19-0.96	0.019-0.030	0.46-0.83	50, 75, 100, 150	0.3	30
				50, 75, 100, 150	0.4	
55	0.19-0.96	0.019-0.030	0.46-0.83	50, 75, 100, 150	0.3	45
				50, 75, 100, 150	0.4	
				50, 100, 150	0.6	
50	0.19-0.96	0.019-0.030	0.46-0.83	50, 75, 100, 150	0.3	60
				50, 100, 150	0.4	
				50, 100, 150	0.6	
55	0.19-0.96	0.019-0.030	0.46-0.83	50, 75, 100, 150	0.3	70
				50, 75, 100, 150	0.4	
				50, 100, 150	0.6	

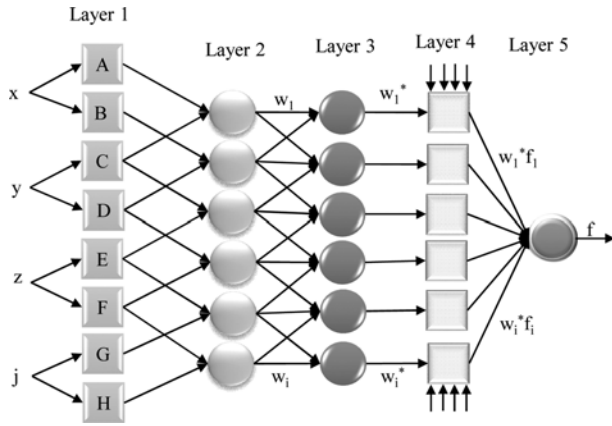


Fig. 2. ANFIS Structure with Four Inputs, One Output and two Rules

$$f(x; a, b, c) = \frac{1}{1 + \left(\frac{x-c}{a}\right)^{2b}} \quad (4)$$

where $\{a, b, c\}$ is the parameter set.

The second layer (membership layer) multiplies the incoming signals from the first layer and sends out the product. Each node output represents the firing strength of a rule or weight as:

$$O_{2,i} = w_i = \mu(x)_i \cdot \mu(x)_{i+1}, i = 1, 2, \dots \quad (5)$$

The third layer (i.e. the rule layer) is non-adaptive, where every node i calculates the ratio of the rule's firing strength to the sum of all rules' firing strengths as

$$O_{3,i} = w_i^* = \frac{w_i}{w_1 + w_2}, i = 1, 2, \dots \quad (6)$$

The outputs of this layer are called normalized firing strengths or normalized weights.

The fourth layer (i.e. the defuzzification layer) provides the output values resulting from the inference of rules, where every node i is an adaptive node with the following node function:

$$O_{4,i} = w_i^* \cdot f_i = w_i^* (p_i x + q_i y + r_i) \quad (7)$$

where $\{p_i, q_i, r_i\}$ is the parameter set, which is referred to as the consequent parameter.

The fifth layer (i.e. the output layer) sums up all the inputs coming from the fourth layer and transforms the fuzzy classification results into a crisp (binary). The single node in the fifth layer is not adaptive, and it computes the overall output as the summation of all incoming signals.

$$O_{5,i} = \sum_i w_i^* \cdot f_i = \frac{\sum_i w_i \cdot f_i}{\sum_i w_i} \quad (8)$$

2.3 Evaluation of Model Performance

To evaluate the performance of the ANFIS models and measured values, the following statistical indicators were selected:

Root Mean Square Error (*RMSE*)

$$RMSE = \sqrt{\frac{\sum_{i=1}^N (o_i - t_i)^2}{N}} \quad (9)$$

Mean Absolute Error (*MAE*)

$$MAE = \frac{1}{N} \sum_{i=1}^N |o_i - t_i| \quad (10)$$

Average absolute deviation (%)

$$\delta = \frac{\sum_{i=1}^N |o_i - t_i|}{\sum_{i=1}^N o_i} \times 100 \quad (11)$$

Nash–Sutcliffe efficiency (*NSE*)

$$NSE = 1 - \frac{\sum_{i=1}^N (t_i - o_i)^2}{\sum_{i=1}^N (t_i - \bar{t})^2} \quad (12)$$

where o_i is an ANFIS value, t_i represents a measured value, and N is the total number of investigated data.

The advantage of the $\delta\%$ statistical error model is that it calculates non-dimensional error in percent, and the advantage of RMSE and MAE is that they investigate the prediction error on the same scale as the output values. Thus, these statistical methods should be considered together. The closer RMSE, MAE and $\delta\%$ are to 0 and the closer *NSE* is to 1, the more accurate the studied model is.

3. Results

3.1 Input Variables

In this study, eight different ANFIS models were run and compared. Each ANFIS model used a different input combination. Table 2 demonstrates the variables of each input combination. This table shows that each input combination consists of some non-dimensional variables. The non-dimensional variables comprise the weir height w , weir length L , main channel width b , weir included angle θ , upstream flow depth y_1 and upstream Froude number Fr_1 . According to Table 2, *Input#1* to *Input#8* have 5, 4, 3, 3, 3, 3, 2 and 1 non-dimensional variables. The goal of

Table 2. Eight Different Input Combinations Investigated

Input combinations	Input variables				
	w/b	y_1/b	L/b	$\sin(\theta/2)$	Fr_1
Input#1	w/b	y_1/b	L/b	$\sin(\theta/2)$	Fr_1
Input#2	w/y_1	L/b	$\sin(\theta/2)$	Fr_1	
Input#3	w/y_1	$L \times \sin(\theta/2)/b$	Fr_1		
Input#4	w/y_1	$L \times Fr_1/b$	$\sin(\theta/2)$		
Input#5	$w \times \sin(\theta/2)/y_1$	L/b	Fr_1		
Input#6	$w \times Fr_1/y_1$	L/b	$\sin(\theta/2)$		
Input#7	$w \times L/(b \times y_1)$	$Fr_1 \times \sin(\theta/2)$			
Input#8	$w \times L \times Fr_1 \times \sin(\theta/2)/(b \times y_1)$				

Table 3. Statistical Parameters for the Non-dimensional Variables

Variable	Statistical parameters				
	Min	Max	Mean	Standard deviation	Variation coefficient
w/b	0.125	0.375	0.241	0.094	0.390
w/y ₁	0.461	0.831	0.671	0.098	0.146
y ₁ /b	0.200	0.513	0.348	0.096	0.275
L/b	0.75	1.5	1.012	0.285	0.281
sin(θ/2)	0.499	0.939	0.769	0.161	0.209
Fr ₁	0.192	1.001	0.438	0.181	0.413
L×sin(θ/2)/b	0.374	1.409	0.705	0.304	0.431
L×Fr ₁ /b	0.150	1.306	0.443	0.229	0.516
w×sin(θ/2)/y ₁	0.234	0.757	0.515	0.131	0.254
w×Fr ₁ /y ₁	0.134	0.607	0.281	0.091	0.323
w×L/(b×y ₁)	0.352	1.247	0.679	0.220	0.324
Fr ₁ ×sin(θ/2)	0.112	0.816	0.334	0.152	0.455
w×L×Fr ₁ ×sin(θ/2)/(b×y ₁)	0.067	0.593	0.219	0.108	0.493

examining the input combinations was to investigate the performance of ANFIS with different input combinations.

The statistical parameters (minimum value, maximum value, mean and standard deviation) for the non-dimensional variables used in the eight input combinations were calculated and presented in Table 3.

3.2 ANFIS Model Analysis

Initially, the ANFIS network was trained with the data measured in the above-mentioned experimental procedure. Three bell-shaped membership functions were used to fuzzify the ANFIS inputs. After the training process, the ANFIS networks were tested to determine the discharge coefficient of the improved triangular side weir. A total of eight ANFIS models were tested in this study. Each ANFIS model used different input combinations. In Table 4, the performance of the ANFIS models in estimating the discharge coefficient was evaluated according to the statistical criteria of RMSE, MAE, δ% and NSE. According to this table, *Input#1*, as the best input combination with five input variables, i.e. w/b, y₁/b, L/b, sin(θ/2) and Fr₁, was significantly more accurate than *Input#8* with only one input variable, i.e. w×L×Fr₁×sin(θ/2)/(b×y₁). Thus, it can be concluded that the ANFIS technique performs significantly better in cases when more but simpler input variables are used.

Table 4. Performance Statistics for the ANFIS Models in Estimating the Discharge Coefficient with Different Statistical Indicators

	RMSE	MAE	%
Input#1	0.014	0.010	1.602
Input#2	0.023	0.017	2.698
Input#3	0.090	0.068	11.304
Input#4	0.044	0.034	5.573
Input#5	0.057	0.044	6.934
Input#6	0.038	0.030	4.748
Input#7	0.084	0.067	10.296
Input#8	0.088	0.068	11.027

According to Table 4, another parameter that directly affects model performance is selecting the appropriate non-dimensional input variables. For example, both *Input#3* and *Input#4* had three input variables. However, *Input#3* had Fr₁ as a separate input variable and sin(θ/2) as a combined input variable. On the other hand, *Input#4* used sin(θ/2) as a separate input variable and Fr₁ as a combined input variable. The results show that *Input#4* had significantly higher performance compared to *Input#1*. This conclusion applies to *Input#5* and *Input#6* as well. The results show that *Input#6* with separate and combined sin(θ/2) as well as Fr₁ input variables exhibited higher modeling precision compared to *Input#5* with combined and separate input variables sin(θ/2) and Fr₁. In addition, by comparing the results of *Input#4* and *Input#6*, it can be concluded that using L/b as a separate input variable can increase modeling performance.

The scatter plots of eight ANFIS models for the test dataset are demonstrated in Fig. 3. The eight models were constructed using eight input combinations, as seen in Table 2. The linear trend line equation for each ANFIS model is shown in each figure. The trend line equation is given as:

$$y = C_1x + C_2 \tag{13}$$

In this equation, the closer C₁ and C₂ are to one and zero, respectively, the more accurate the model is. From Fig. 3, it is obvious that the ANFIS model with *Input#1* was significantly more efficient than the other ANFIS models, and the trend line of this model almost fits the exact line.

As seen in Fig. 3, the ANFIS models with *Input#1* and *Input#2* are not trapped in over or underestimation. However, other ANFIS models are trapped in overestimation when the discharge coefficient is lower than the mean value, or they are trapped in underestimation when the discharge coefficient is higher than the mean.

The NSE values for eight ANFIS models are presented in Fig. 4. It should be noted that NSE takes a value between -∞ and 1. NSE of 1 indicates an exact match between the ANFIS model and the experimental results; NSE of 0 shows that the efficiency

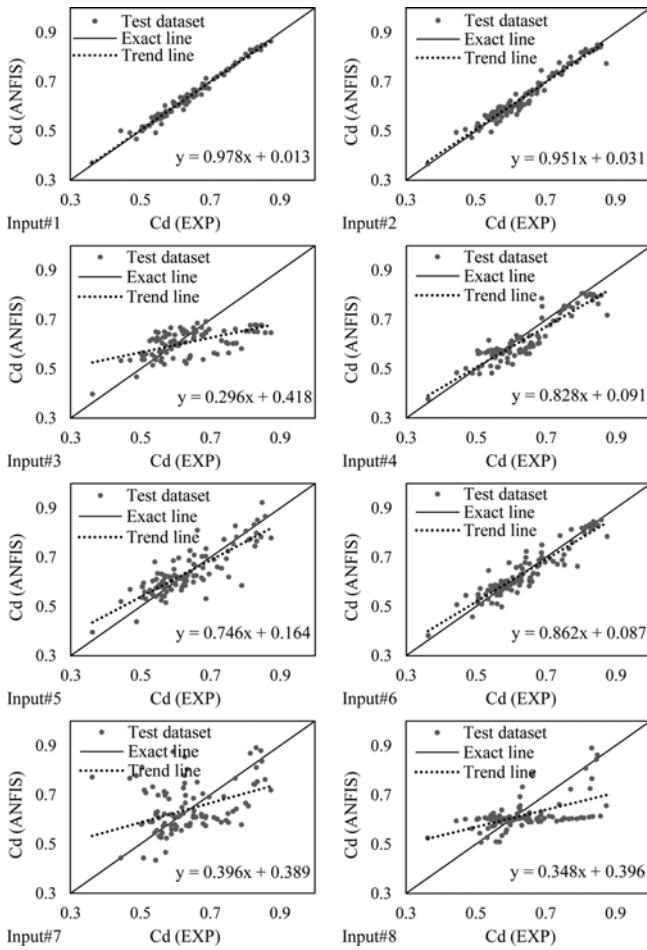


Fig. 3. Scatter Plots of Values Predicted by the ANFIS Models

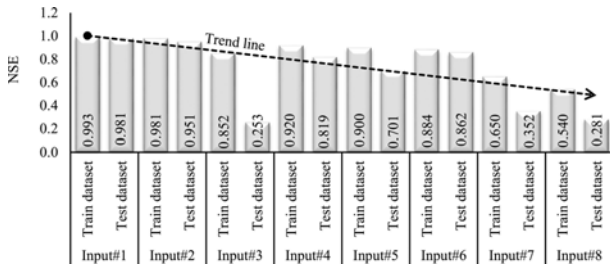


Fig. 4. NSE in the Testing and Training Phases of the ANFIS Models

of the ANFIS model is similar to the mean experimental results, and *NSE* of less than 0 indicates that the mean experimental result is a better repressor compared to the ANFIS model. From this figure, two major ideas are derived:

(i) A more similar *NSE* value for the testing and training datasets indicates that the ANFIS models were not over-trained. Overtraining occurs when the accuracy of the testing process is significantly lower than training.

(ii) Considering the trend line, it can be concluded that the performance of the ANFIS models decreases with a lower number of input variables. It can be seen that ANFIS with *Input#1* and *Input#2* (five and four input variables, respectively) significantly outperformed ANFIS with *Input#7* and *Input#8* (two and one

input variables, respectively).

3.3 ANFIS Model Verification

The best ANFIS model with *Input#1* was compared with the soft computing and regression models. Eq. (14) represents the particle swarm optimization conducted by Zaji and Bonakdari (2014) to estimate the discharge coefficient of an improved triangular side weir. Eq. (15) shows the nonlinear regression-based equation introduced by Borghei and Parvaneh (2011) to calculate the discharge coefficient for an improved triangular side weir.

$$Cd = 1.030 - 0.264 \left(\frac{w}{L}\right)^{0.353} - 0.363 \left(\frac{Fr_1}{\sin(\theta/2)}\right)^{0.901} + 1.484 \left(\frac{w}{y_1}\right)^{1.057} - 1.773 \left(\frac{w \sin(\theta/2)}{y_1}\right)^{0.933} \quad (14)$$

$$Cd = \left[-0.18 \left(\frac{Fr_1}{\sin(\theta/2)}\right)^{0.71} - 0.15 (Fr_1)^{0.44} + \left(\frac{w}{y_1}\right)^{0.7} \right] \times \left[-2.37 + 2.58 \left(\frac{w \sin(\theta/2)}{y_1}\right) \right] \quad (15)$$

The comparison is displayed as a residual scatter plot (Fig. 5). The horizontal axis in this figure shows the residual of the discharge coefficient (predicted and experimental results) and the vertical axis shows the experimental discharge coefficient value. The $2 \times$ standard deviation (*SD*) interval is shown in this figure. *SD* is defined by Eq. (16).

$$SD = \sqrt{\frac{1}{N-1} \sum_{i=1}^N (\text{Res}_i - \overline{\text{Res}})^2} \quad (16)$$

where *N* is the number of samples, Res_i is the residual of predicted-examined sample *i*, and $\overline{\text{Res}}$ is the average of the

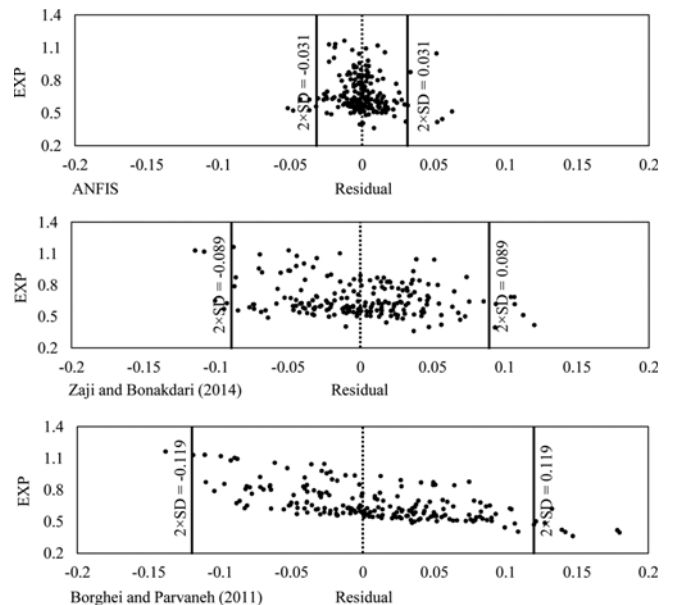


Fig. 5. Comparison between the Residual Scatter Plot of the ANFIS Model and Previous Studies

residuals of the entire dataset calculated by the following equations:

$$\text{Res}_i = t_i - o_i \quad (17)$$

$$\overline{\text{Res}} = \frac{1}{N} \sum_{i=1}^N \text{Res}_i \quad (18)$$

where o_i is the i^{th} output of the numerical models and t_i is the i^{th} experimental result.

Nearly 95% of the entire dataset is located within the $-2 \times SD$ to $2 \times SD$ interval. Fig. 5 indicates that 95% of the ANFIS-predicted samples are between the 0.031 and -0.031 residual. However, this value was between 0.089 and -0.089 for Zaji and Bonakdari (2014) and between 0.119 and -0.119 for Borghei and Parvaneh's (2011) equations. Therefore, it can be concluded that ANFIS can predict the side weir discharge coefficient with three and four times more accuracy than Zaji and Bonakdari's (2014) method and Borghei and Parvaneh's (2011) equation, respectively.

4. Conclusions

The adaptive neuro-fuzzy technique was applied in this study to simulate the discharge coefficient of an improved triangular side weir. The models were constructed using eight different input combinations. A comparison of the ANFIS models developed indicated that the input combinations with more, yet simpler input variables were significantly more accurate compared to the input combinations with less but more complex input variables. Thus, in terms of the w/b , y_1/b , L/b , $\sin(\theta/2)$ and Fr_1 input variables, the ANFIS model with $RMSE$, MAE and $\delta\%$ of 0.014, 0.01, and 1.602, respectively, was selected as the model with the highest performance. Finally, the best ANFIS model obtained in the present study was compared with results from two previous studies by Zaji and Bonakdari (2014) and Borghei and Parvaneh (2011). According to the results, the ANFIS model with a $2 \times SD$ value of 0.031 was significantly more accurate than Zaji and Bonakdari (2014) and Borghei and Parvaneh's (2011) findings with $2 \times SD$ of 0.089 and 0.119, respectively.

References

- Aydin, M. C. and Emiroglu, M. E. (2013). "Determination of capacity of labyrinth side weir by CFD." *Flow Meas. Instrum.*, Vol. 29, No. 2013, pp. 1-8, DOI: 10.1016/j.flowmeasinst.2012.09.008.
- Bilhan, O., Emiroglu, M. E., and Kisi, O. (2010). "Application of two different neural network techniques to lateral outflow over rectangular side weirs located on a straight channel." *Adv. Eng. Software*, Vol. 41, No. 6, pp. 831-837, DOI: 10.1016/j.advengsoft.2010.03.001.
- Bilhan, O., Emiroglu, M. E., and Kisi, O. (2011). "Use of artificial neural networks for prediction of discharge coefficient of triangular labyrinth side weir in curved channels." *Adv. Eng. Software*, Vol. 42, No. 4, pp. 208-214, DOI: 10.1016/j.advengsoft.2011.02.006.
- Borghei, S. M. and Parvaneh, A. (2011). "Discharge characteristics of a modified oblique side weir in subcritical flow." *Flow Meas. Instrum.*, Vol. 22, No. 5, pp. 370-376, DOI: 10.1016/j.flowmeasinst.2011.04.009.
- Cosar, A. and Agaccioglu, H. (2004). "Discharge coefficient of a triangular side-weir located on a curved channel." *J. Irrig. Drain. Eng.*, Vol. 130, No. 5, pp. 410-423, DOI: 10.1061/(ASCE)0733-9437(2004)130:5(410).
- Dastorani, M. T., Afkhami, H., Sharifidarani, H., and Dastorani, M. (2010). "Application of ANN and ANFIS models on dryland precipitation prediction (case study: Yazd in central Iran)." *J. Appl. Sci.*, Vol. 10, No. 20, pp. 2387-2394, DOI: 10.3923/jas.2010.2387.2394.
- De Marchi, G. (1934). "Saggio di teoria del funzionamento degli stramazzi laterali." *L'Energia Elettrica*, Vol. 11, No. 11, pp. 849-860.
- Dursun, O. F., Kaya, N., and Firat, M. (2012). "Estimating discharge coefficient of semi-elliptical side weir using ANFIS." *J. Hydrol.*, Vols. 426-427, No. 2012, pp. 55-62, DOI: 10.1016/j.jhydrol.2012.01.010.
- Ebtehaj, I. and Bonakdari, H. (2014). "Performance evaluation of adaptive neural fuzzy inference system for sediment transport in sewers." *Water Resour. Manage.*, Vol. 28, No. 13, pp. 4765-4779, DOI: 10.1007/s11269-014-0774-0.
- El-Shafie, A., Jaafer, O., and Seyed, A. (2011). "Adaptive neuro-fuzzy inference system based model for rainfall forecasting in Klang River, Malaysia." *Int. J. Phys. Sci.*, Vol. 6, No. 12, pp. 2875-2888.
- Emiroglu, M. E. and Kisi, O. (2013). "Prediction of discharge coefficient for trapezoidal labyrinth side weir using a neuro-fuzzy approach." *Water Resour. Manage.*, Vol. 27, No. 5, pp. 1473-1488, DOI: 10.1007/s11269-012-0249-0.
- Emiroglu, M. E., Kisi, O., and Bilhan, O. (2010). "Predicting discharge capacity of triangular labyrinth side weir located on a straight channel by using an adaptive neuro-fuzzy technique." *Adv. Eng. Software*, Vol. 41, No. 2, pp. 154-160, DOI: 10.1016/j.advengsoft.2009.09.006.
- Ghodsian, M. (2003). "Supercritical flow over a rectangular side weir." *Can. J. Civ. Eng.*, Vol. 30, No. 3, pp. 596-600, DOI: 10.1139/L03-004.
- Ghodsian, M. (2004). "Flow over triangular side weir." *Sci. Iranica*, Vol. 11, Nos. 1-2, pp. 114-120.
- Jang, J. S. R. (1993). "ANFIS: Adaptive-network-based fuzzy inference system." *IEEE Trans. Syst. Man. Cybern.*, Vol. 23, No. 3, pp. 665-685, DOI: 10.1109/21.256541.
- Khajeh, A., Modarress, H., and Rezaee, B. (2009). "Application of adaptive neuro-fuzzy inference system for solubility prediction of carbon dioxide in polymers." *Expert. Sys. Appl.*, Vol. 36, No. 3 PART 1, pp. 5728-5732, DOI: 10.1016/j.eswa.2008.06.051.
- Kisi, O., Bilhan, O., and Emiroglu, M. E. (2013). "Anfis to estimate discharge capacity of rectangular side weir." *Proc. Inst. Civ. Eng. Water Manage.*, Vol. 166, No. 9, pp. 479-487, DOI: 10.1680/wama.11.00095.
- Kisi, O., Emin Emiroglu, M., Bilhan, O., and Guven, A. (2012). "Prediction of lateral outflow over triangular labyrinth side weirs under subcritical conditions using soft computing approaches." *Expert. Sys. Appl.*, Vol. 39, No. 3, pp. 3454-3460, DOI: 10.1016/j.eswa.2011.09.035.
- Kumar, C. P. and Pathak, S. K. (1987). "Triangular side weirs." *J. Irrig. Drain. Eng.*, Vol. 113, No. 1, pp. 98-105, DOI: 10.1061/(ASCE)0733-9437(1987)113:1(98).
- Mirnaseri, M. and Emadi, A. (2013). "Hydraulic performance of combined flow rectangular labyrinth weir-gate." *Middle. East. J. Sci. Res.*, Vol. 18, No. 9, pp. 1335-1342, DOI: 10.5829/idosi.mejrs.2013.18.9.12374.
- Muslu, Y. (2001). "Numerical analysis of lateral weir flow." *J. Irrig. Drain. Eng.*, Vol. 127, No. 4, pp. 246-253, DOI: 10.1061/(ASCE)0733-9437(2001)127:4(246).
- Muslu, Y., Tozlu, H., and Yuksel, E. (2003). "Effect of lateral water surface profile on side weir discharge." *J. Irrig. Drain. Eng.*, Vol. 129, No. 5, pp. 371-375, DOI: 10.1061/(ASCE)0733-9437(2003)

- 129:5(371).
- Nadesamoorthy, T. and Thomson, A. (1972). "Discussion of" Spatially Varied Flow over Side-Weirs". *J. Hydraul. Div.*, Vol. 98, No. 12, pp. 2234-2235.
- Onen, F. (2014a). "GEP prediction of scour around a side weir in curved channel." *J. Environ Eng. Landsc. Manage.*, Vol. 22, No. 3, pp. 161-170, DOI: 10.3846/16486897.2013.865632.
- Onen, F. (2014b). "Prediction of scour at a side-weir with GEP, ANN and Regression Models." *Arab. J. Sci. Eng.*, Vol. 39, No. 8, pp. 6031-6041, DOI: 10.1007/s13369-014-1244-y.
- Petković, D. and Čojbašić, Z. (2011). "Adaptive neuro-fuzzy estimation of automatic nervous system parameters effect on heart rate variability." *Neural. Comput. Appl.*, Vol. 21, No. 8, pp. 2065-2070. DOI: 10.1007/s00521-011-0629-z.
- Petković, D., Čojbašić, Ž., and Lukić, S. (2013a). "Adaptive neuro fuzzy selection of heart rate variability parameters affected by autonomic nervous system." *Expert. Sys. Appl.*, Vol. 40, No. 11, pp. 4490-4495, DOI: 10.1016/j.eswa.2013.01.055.
- Petković, D., Issa, M., Pavlović, N. D., Pavlović, N. T., and Zentner, L. (2012). "Adaptive neuro-fuzzy estimation of conductive silicone rubber mechanical properties." *Expert. Sys. Appl.*, Vol. 39, No. 10, pp. 9477-9482, DOI: 10.1016/j.eswa.2012.02.111.
- Petković, D., Pavlović, N. D., Čojbašić, Ž., and Pavlović, N. T. (2013b). "Adaptive neuro fuzzy estimation of underactuated robotic gripper contact forces." *Expert. Sys. Appl.*, Vol. 40, No. 1, pp. 281-286, DOI: 10.1016/j.eswa.2012.07.076.
- Ranga Raju, K. G., Prasad, B., and Gupta, S. K. (1979). "Side weir in rectangular channel." *J. Hydraul. Div.*, Vol. 105, No. 5, pp. 547-554.
- Seyedian, S. M., Ghazizadeh, M. J., and Tareghian, R. (2014). "Determining side-weir discharge coefficient using Anfis." *Proc. Inst. Civ. Eng. Water Manage.*, Vol. 167, No. 4, pp. 230-237, DOI: 10.1680/wama.12.00102.
- Singh, R., Manivannan, D., and Satyanarayana, T. (1994). "Discharge coefficients of rectangular side weirs." *J. Irrig Drain. Eng.*, Vol. 120, No. 4, pp. 814-819, DOI: 10.1061/(ASCE)0733-9437(1996)122:2(132).
- Swamee, P. K., Pathak, S. K., and Ali, M. S. (1994). "Side weir analysis using elementary discharge coefficient." *J. Irrig. Drain. Eng.*, Vol. 120, No. 4, pp. 742-755, DOI: 10.1061/(ASCE)0733-9437(1994)120:4(742).
- Talei, A., Chua, L. H. C., and Quek, C. (2010). "A novel application of a neuro-fuzzy computational technique in event-based rainfall-runoff modeling." *Expert. Sys. Appl.*, Vol. 37, No. 12, pp. 7456-7468, DOI: 10.1016/j.eswa.2010.04.015.
- Wahida Banu, R. S. D., Shakila Banu, A., and Manoj, D. (2011). "Identification and control of nonlinear systems using soft computing techniques." *Int. J. Model. Optimiz.*, Vol. 1, No. 1, pp. 24-28, DOI: 10.7763/IJMO.2011.V1.5.
- Wu, C. L. and Chau, K. W. (2012). "Prediction of rainfall time series using modular soft computing methods." *Eng. Appl. Artif. Intell.*, Vol. 26, No. 3, pp. 997-1007, DOI: 10.1016/j.engappai.2012.05.
- Yuksel, E. (2004). "Effect of specific energy variation on lateral overflows." *Flow Meas Instrum.*, Vol. 15, Nos. 5-6, pp. 259-269, DOI: 10.1016/j.flowmeasinst.2004.06.005.
- Zaji, A. H. and Bonakdari, H. (2014). "Performance evaluation of two different neural network and particle swarm optimization methods for prediction of discharge capacity of modified triangular side weirs." *Flow. Meas. Instrum.*, Vol. 40, pp. 149-156, DOI: 10.1016/j.flowmeasinst.2014.10.002.